Polarimetric Detection Scheme for Passive Radar based on a 2D Auto-Regressive Disturbance Model

Francesca Filippini, Fabiola Colone
Dept. of Information Engineering, Electronics and Telecommunications (DIET),
Sapienza University of Rome, Via Eudossiana, 18 - 00184 Rome, Italy
{francesca.filippini, fabiola.colone}@uniroma1.it

***Abstract* —Suitable strategies to exploit polarimetric diversity have been proved to be able to enhance the target detection capability of passive radar (or passive coherent location - PCL) systems. In this work, the authors describe a novel polarimetric adaptive detection scheme, based on a two-dimensional auto-regressive model for the disturbance. The effectiveness of the proposed strategy is shown against experimental data collected by means of a FM radio based multi-channel PCL prototype. The obtained results are also compared with alternative polarimetric detection schemes in order to provide a first insight into the benefits of the newly proposed solution.**

Index Terms — passive radar, target detection, polarimetric diversity, FM radio signals, two-dimensional auto-regressive model.

I. Introduction

Over the last two decades, a significant amount of contributions in the open literature has been dedicated to passive radar (PR or *passive coherent location* – PCL) technology. Given the wide interest in this matter [1]-[2], target detection and localization capability has considerably improved. However, despite the effectiveness of the devised processing techniques, a variety of disturbance contributions might still limit the performance of PCL systems. With particular reference to a FM radio based PCL system, the major disturbance sources, other than the direct signal from the transmitter and its multipath replicas, are represented by co/adjacent-channel interferences [3], [4], typically due to frequency reuse or broad-spectrum roll-off.

In the recent years, the exploitation of polarimetric diversity has been considered and proved to be able to effectively increase the system reliability against those effects that are not under the control of the PCL radar designer [5]-[10].

A first attempt toward this direction has been presented in [5], where a non-coherent integration (NCI) of the range-Doppler maps obtained from two orthogonally polarized surveillance antennas was considered. A more effective strategy was used in [7] and [8], where a polarimetric locally adaptive detection scheme was devised based on a generalized likelihood ratio test (GLRT) applied over the range-Doppler domain. This approach, referred to as the Pol-GLRT, has been shown to be able to adaptively exploit the polarimetric differences between the target and the competing disturbance, thus successfully mitigating the effects of the interferences and significantly improving the target detection performance of the system. Note that this approach adaptively operates on the polarimetric domain only.

In [9], an alternative solution was proposed by considering the possibility of globally adapting the weights of the polarimetric whitening filter in the time domain. The authors have shown that, under some simplifying assumptions on the disturbance, this approach can provide a reasonable tradeoff between achievable performance and computational complexity. However, this approach shows its limitations against scenarios where the disturbance correlation in the time domain cannot be neglected. The latter consideration suggests the possibility to adaptively jointly exploit the polarimetric and temporal domain.

In this work, we derive a novel model-based polarimetric adaptive detection scheme. To this end, after the conventional cancellation stage aimed at reducing the direct signal, clutter and multipath contributions, we model the residual disturbance affecting the surveillance signals as a two-dimensional (2D) auto-regressive (AR) process and exploit this model to develop a target detection scheme. We investigate the effectiveness of the proposed approach against the same experimental data set used in [7] to enable a comparison with previously considered polarimetric detection schemes.

The paper is organized as follows. In Section II, we present the proposed polarimetric adaptive detection scheme for a FM radio-based PCL system. In Section III an experimental validation is carried out on the available data set and the performance are compared with previously proposed approaches. Finally, our future research outlook is described in Section IV and some conclusions are drawn in Section V.

II. Auto-regressive Model Based Polarimetric Adaptive Detection Scheme

Let us consider a FM radio-based PCL system, equipped with L receiving channels, connected to differently polarized surveillance antennas.

According to the processing scheme introduced in [7], the signals collected by different antennas separately undergo the

978-1-7281-2660-9/19/$31.00 ©2019 IEEE

disturbance (direct signal and multipath) cancellation stage. Depending on the availability of one or more differently polarized reference antennas, this stage can be performed according to either the Extensive Cancellation Algorithm (ECA) [11] or its polarimetric version (P-ECA) [7].

Once this stage has been performed, L sequences of samples are made available corresponding to the polarimetric channels deployed. We arrange the L outputs extracted at the m-th time lag into an L-dimensional vector $\mathbf{x}(m) = [x_0(m) \dots x_l(m) \dots x_{L-1}(m)]^T$ $(m = 0, \dots, N-1)$, being N the number of samples in the exploited coherent processing interval (CPI). Vector $\mathbf{x}(m)$ can be written as

$$\mathbf{x}(m) = \gamma\, \boldsymbol{\alpha}\, s(m) + \mathbf{d}(m) \tag{1}$$

where $\gamma = 0$ $(\gamma = 1)$ under the null H_0 (alternate H_1) hypothesis; $\boldsymbol{\alpha} = [\alpha_0 \dots \alpha_l \dots \alpha_{L-1}]^T$ is the vector of unknown target complex amplitudes at different polarimetric channels, assumed constant during the CPI; $s(m)$ is the m-th sample of the transmitted signal, delayed in time by τ and Doppler shifted by f_d; $\mathbf{d}(m)$ is the $(L \times 1)$ disturbance vector extracted at the m-th time lag.

Along with thermal noise, the disturbance vector might include interference from other transmissions at co-/adjacent channels as well as residual clutter contributions. We model it as a 2D AR model of order $(Q-1)$ and matrix parameters $\mathbf{A}$ and $\mathbf{R}$

$$\mathbf{d}(m) = \sum_{q=1}^{Q-1} \mathbf{A}^H(q)\mathbf{d}(m-q) + \mathbf{w}(m) \tag{2}$$

where $\mathbf{A} = [\mathbf{A}^H(Q-1)\ \mathbf{A}^H(Q-2)\ \dots\ \mathbf{A}^H(1)]^H$ denotes the $(L(Q-1) \times L)$ matrix of 2D AR parameters and $\mathbf{w}(m)$ is a sample from a white vectorial complex Gaussian process with zero mean and covariance matrix $\mathbf{R}$ $(L \times L)$.

Based on this model, the joint probability density function (pdf) of the data vectors under the H_0 hypothesis can be written as

$$f_0\left(\mathbf{x} \middle| \mathbf{R}, \{\mathbf{A}(q)\}_{q=1}^{Q-1}\right) = (\pi^L|\mathbf{R}|)^{-(N-Q+1)} \times \exp\left\{-\sum_{m=Q}^{N}\left(\mathbf{x}(m) - \sum_{q=1}^{Q-1}\mathbf{A}^H(q)\mathbf{x}(m-q)\right)^H \mathbf{R}^{-1}\left(\mathbf{x}(m) - \sum_{q=1}^{Q-1}\mathbf{A}^H(q)\mathbf{x}(m-q)\right)\right\} \tag{3}$$

To simplify the notation, we can rearrange the data into matrix

$$\mathbf{X} = [\tilde{\mathbf{x}}(0)\ \tilde{\mathbf{x}}(1) \dots \tilde{\mathbf{x}}(N-Q)] \tag{4}$$

where $\tilde{\mathbf{x}}(m) = [\mathbf{x}(m)^T \dots \mathbf{x}(m+Q-1)^T]^T$. Using this definition, the pdf of $\mathbf{X}$ under the H_γ hypothesis is written as

$$f_\gamma(\mathbf{X}|\ \gamma\boldsymbol{\alpha}, \mathbf{R}, \mathbf{A}) = (\pi^L|\mathbf{R}|)^{-(N-Q+1)} e^{\{-\mathrm{tr}[(\mathbf{X}-\gamma\mathbf{S})^H \mathbf{P}\, (\mathbf{X}-\gamma\mathbf{S})]\}} \tag{5}$$

being $\mathbf{P} = [\mathbf{H}^H\mathbf{R}^{-1}\mathbf{H}]$, $\mathbf{H} = [-\mathbf{A}^H \quad \mathbf{I}_L]$ and $\mathbf{S}$ the target matrix, obtained by applying the same reordering operation as for $\mathbf{X}$.

To derive the sought target detection scheme, we resort to a two-stage approach.
First, we derive the detection test assuming that the disturbance characteristics, namely $\mathbf{A}$ and $\mathbf{R}$ matrices, are known; then we plug into the derived test suitable estimates of these parameters.

Specifically, we write the GLRT with respect to the unknown target amplitude vector $\boldsymbol{\alpha}$:

$$\frac{\max_{\boldsymbol{\alpha}}\{f_1(\mathbf{X}|\ \boldsymbol{\alpha}, \mathbf{R}, \mathbf{A})\}}{f_0(\mathbf{X}|\mathbf{R}, \mathbf{A})} \underset{H_0}{\overset{H_1}{\gtrless}} \eta_0 \tag{6}$$

where η_0 is the detection threshold. Maximizing the above expression over $\boldsymbol{\alpha}$ and after some algebraic manipulations, we obtain:

$$\sum_{m=0}^{N-Q} \tilde{\mathbf{x}}^H(m)\, \mathbf{P}\, \boldsymbol{\Sigma}(m) \left[\sum_{m=0}^{N-Q} \boldsymbol{\Sigma}^H(m)\mathbf{P}\, \boldsymbol{\Sigma}(m)\right]^{-1} \times \sum_{m=0}^{N-Q} \boldsymbol{\Sigma}^H(m)\, \mathbf{P}\ \tilde{\mathbf{x}}(m) \underset{H_0}{\overset{H_1}{\gtrless}} \eta_0 \tag{7}$$

where $\boldsymbol{\Sigma}(m) = \tilde{\mathbf{s}}(m) \otimes \mathbf{I}_L$, $\tilde{\mathbf{s}}(m) = [s(m) \dots s(m-Q+1)]^T$.

In order to obtain suitable estimates of matrices $\mathbf{A}$ and $\mathbf{R}$, we assume that the target contribution in the CPI is negligible with respect to the competing background. Therefore, we can make use of the data $\mathbf{X}$ itself to obtain the estimated covariance matrix $\widehat{\mathbf{Q}} = \mathbf{X}\mathbf{X}^H$, from which the maximum likelihood (ML) estimates of $\mathbf{A}$ and $\mathbf{R}$ are obtained as follows:

$$\begin{gathered}\widehat{\mathbf{A}} = \widehat{\mathbf{Q}}_{00}^{-1}\widehat{\mathbf{Q}}_{01} \\ \widehat{\mathbf{R}} = \frac{1}{(N-Q+1)}\left[\widehat{\mathbf{Q}}^{-1}\right]_{Q,Q}^{-1}\end{gathered} \tag{8}$$

where $\left[\widehat{\mathbf{Q}}^{-1}\right]_{Q,Q}^{-1}$ is the last $(L \times L)$ block of the principal diagonal of the inverse of $\widehat{\mathbf{Q}}$ while $\widehat{\mathbf{Q}}_{00}$ and $\widehat{\mathbf{Q}}_{01}$ are $(L(Q-1) \times L(Q-1))$ and $(L(Q-1) \times L)$ blocks of $\widehat{\mathbf{Q}}$, namely

$$\widehat{\mathbf{Q}} = \mathbf{X}\mathbf{X}^H = \begin{bmatrix}\widehat{\mathbf{Q}}_{00} & \widehat{\mathbf{Q}}_{01} \\ \widehat{\mathbf{Q}}_{01}^{\mathrm{H}} & \widehat{\mathbf{Q}}_{11}\end{bmatrix} \tag{9}$$

Now, by substituting (8) in (7), a practical detection test is obtained. In the following, it will be referred to as AR model based Polarimetric Adaptive Matched Filter (Pol-AR-AMF). Note that the derived detector does not guarantee the desired constant false alarm rate (CFAR) property. Therefore, the detection threshold is scaled according to a conventional Cell Average (CA)-CFAR thresholding.

Moreover, a proper selection of the employed parameter Q must be carried out. In fact, since the AR model order ultimately depends on the disturbance correlation characteristics, its value will have a major impact on the capability to reject it. Additional details on the derivation of the detector and the selection of parameter Q will be reported in an extended journal paper that is currently in preparation.

Finally, we observe that, if $Q = 1$, the derived Pol-AR-AMF corresponds to the approach proposed in [9].

III. EXPERIMENTAL VALIDATION

A. *Experimental data*

In this work, the same data set used in [7] has been considered for the analysis. The acquisition campaign has been conducted near Fiumicino Airport, in Italy, exploiting a FM radio transmitter located in Monte Cavo, approx. 35 km from the receiver site. Two dual-polarized log periodic antennas were used (see Fig.1(a)), being each one equipped with two independent, one vertical (V) one horizontal (H) polarized, outputs.

Specifically, one of them was steered toward the exploited transmitter (TX) of opportunity and employed to collect the V and H polarized versions of the reference signal. The other antenna was pointed toward the area to be monitored and the two outputs gathered the V and H polarized versions of the surveillance signal. The data set consists of 2060 sequential data files (approx. 80 minutes covered), each one containing a 1.1 s registration of the signals simultaneously collected by different antennas at different carrier frequencies. The employed PCL prototype is based on a direct RF sampling approach and exploits the ICS-554 PMC module (GE Fanuc Embedded Systems) (see Fig.1(b)).

This module consists of four 14-bit ADCs sampling synchronously the properly amplified and filtered analogue signals from up to four input channels.

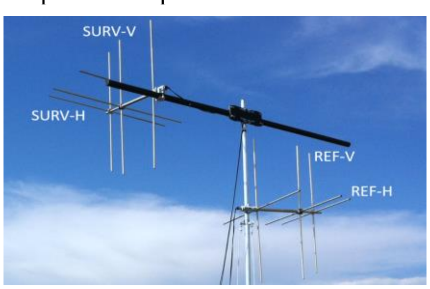

(a)

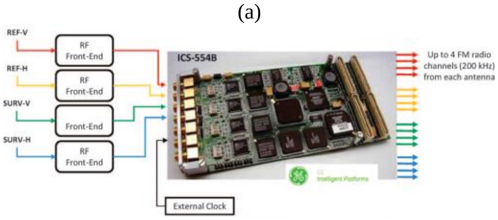

(b)

Fig.1 Acquisition Campaign equipment:
(a) Dual-polarized antennas; (b) Multi-channel PCL prototype

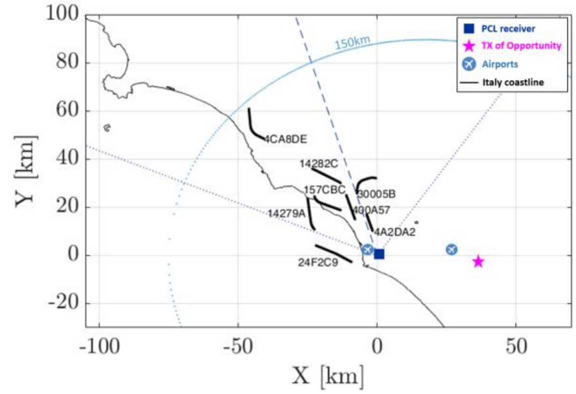

(a)

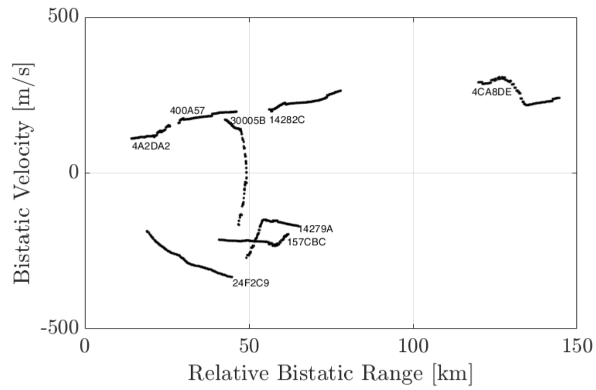

(b)

Fig.2 Air-truth of targets of opportunity projected into the
(a) X-Y plane and (b) bistatic range – bistatic velocity plane.

Simultaneous down conversion of up to 16 arbitrary signal bands (e.g. 16 FM radio channels) is provided by four Graychip GC4016 quad digital down-converters (DDC).

The described setup allows collecting data from up to four different FM radio channels each one from four different antennas. In this paper, we consider the FM channel at 92.4 MHz. The air-truth for the same air space has been provided by the SBS-1 real time virtual radar, a portable low-cost Mode-S/ADS-B receiver.

B. *Experimental Results*

In order to investigate the effectiveness of the proposed detection scheme, we consider 40 consecutive data files. In Fig.2, we report in black the air-truth corresponding to the targets of opportunity that were present at the time. Specifically, Fig.2(a) shows the acquisition geometry and the targets trajectories in the X-Y plane. The dashed and dotted dark blue lines denotes the surveillance antennas steering and main beam, respectively. Additionally, the iso-bistatic range ellipse at 150 km is reported in light blue dots. The same trajectories projected into the bistatic range – bistatic velocity plane, are sketched in Fig.2 (b).

In Fig.3, we report the results obtained for a single data file among the considered set. In Fig.3(a-b) we perform a conventional single-pol processing scheme, in Fig.3(c) we

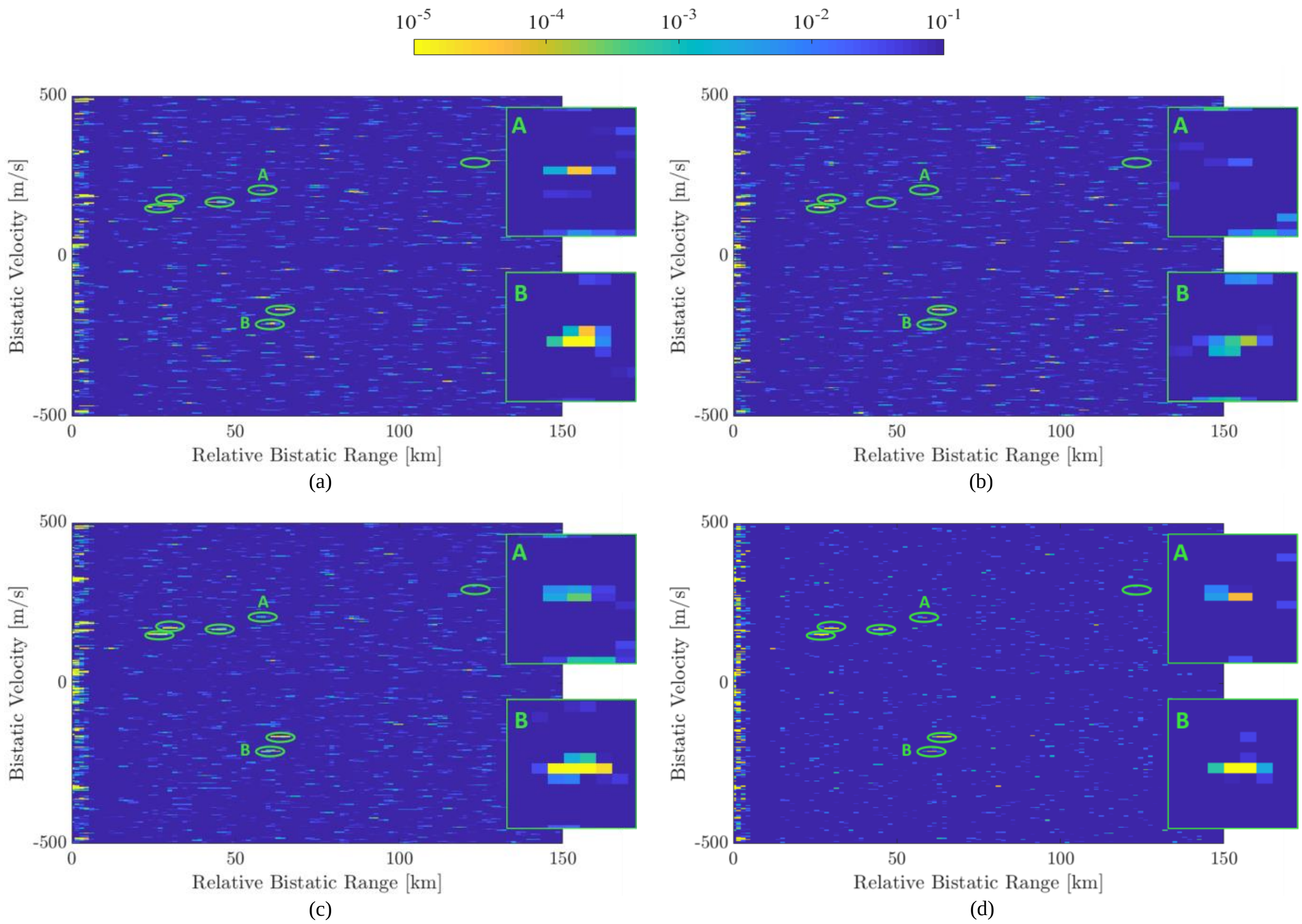

Fig.3 Minimum nominal P_{FA} value to set in order to detect each bin, using
(a) single-pol channel H; (b) single-pol channel V; (c) Pol-GLRT; (d) Pol-AR-AMF with $Q = 5$

show the results obtained when adaptively rejecting the disturbance in the polarimetric domain according to the Pol-GLRT approach [7], while in Fig.3(d) we used the proposed Pol-AR-AMF with $Q = 5$. Specifically, for each case, we report the test statistics over the bistatic range-velocity plane before the application of a proper threshold, selected according to a desired value of nominal P_{FA}. For a fair comparison, the test statistic is mapped into the P_{FA} setting that would allow the corresponding threshold exceeding. In other words, each pixel in the map has been scaled so that it represents the minimum value of nominal P_{FA} to be set for that pixel to yield a detection.

Additionally, all targets that were present at the time of the considered data file are marked with green circles and an enlarged view of targets labelled as A and B is reported next to each figure. We recall that, when exploiting a single-pol channel, the considered surveillance signal undergoes the disturbance cancellation stage and the following evaluation of the Cross-Ambiguity Function (CAF) with the reference signal over the CPI. Consequently, a CA-CFAR would be performed for the detection stage. Notice that we used $M = 32$ secondary data surrounding the CUT, both for the Pol-GLRT, the CA-CFAR used in the Pol-AR-AMF and the CA-CFAR used for the single-pol cases.

Observing Fig.3, the following considerations are in order:

i. The signals received at the two single-pol channels (a-b) and processed according to a conventional single-pol scheme, lead to different results. For instance, targets A and B would be detected with very low P_{FA} only when using the H-pol channel (Fig.3(a)). However, this is not a general result since, depending on the complex structure of the target, the signal polarization may change in the reflection or not, as shown in [7]-[8]. Incidentally, we notice that the exploited TX of opportunity uses V polarization. Moreover, even when strong echoes are received, they are likely to be surrounded by equally strong peaks that do not correspond to any target i.e. a considerably high number of false alarms throughout the considered range-velocity area should be accepted in order to guarantee a good target detection capability.

ii. When both polarization are jointly exploited according to the Pol-GLRT detection scheme (see Fig.3(c)), a strong peak is visible for target B, meaning it would be detected also for quite low nominal P_{FA} values. On the other hand, only a weak echo is received from target A. Moreover, even tough the level of several additional peaks is reduced thanks to an adaptive rejection of the disturbance based on the polarimetric information, the detection scheme would still not be able to offer a good control of the false alarm rate at this data file.

iii. Eventually, when using the proposed Pol-AR-AMF strategy with $Q = 5$ as in Fig.3(d)), low nominal P_{FA} values could be set while still guaranteeing the detection of both targets A and B. Additionally, the proposed detection scheme is able to effectively counteract the disturbance, thus strongly decreasing the background level with respect to all strategies considered above.

iv. Neither of the aforementioned strategies would allow the detection of the target at approximately 130 km at the considered scan. It is worth noticing that this aircraft was rapidly manuveruing and decreasing its altitude while approaching Fiumicino Airport.

The raw detections for the 40 consecutive data files are reported in Fig.4 and Fig.5 for $P_{FA} = 10^{-4}$. In each figure, the available air-truth is reported in black, the grey dots represent all the raw PCL detections while the red dots represent the detections that have been correctly correlated with the air-truth. Specifically, the results obtained with the single-pol channels H and V are shown in Fig.4 (a) and (b), respectively while Fig.5(a) reports the results obtained using the Pol-NCI, Fig.5(b) shows the results obtained with the Pol-GLRT and Fig.5(c) shows the results obtained when performing the proposed Pol-AR-AMF strategy with $Q = 5$.

By observing Fig.4 the same consideration made on Fig.3 can be confirmed. Specifically, the use of a single-pol-operation leads to quite different results depending on the employed polarization. For instance, differences are particularly evident on the target track that rapidly crosses the zero-Doppler at approx. 50 km. However, identifying the best performing single-pol could be a difficult task as the H-pol and the V-pol channels yield performance that might vary with the considered target.

When a simple NCI [5] across the polarimetric channels is performed (see Fig.5(a)) the target detection capability is not enhanced, confirming that the resulting signal to disturbance ratio does not improve because of a corresponding increase in the interference background level. In fact, also some missed detections are obtained at scans where either the H or the V single-pol channel provides correct detections.

Several additional detections are obtained when the two available polarimetric channels are jointly processed according to the Pol-GLRT [7] (Fig.5(b)) and the Pol-AR-AMF (Fig.5(c)) strategies, confirming that not only the advantage of jointly using the two polarimetric channels is due to the integration gain but also this information diversity, if properly exploited, allows an effective disturbance rejection. However, the proposed strategy (Fig.5(c)) offers the best detection performance with respect to all the considered approaches.

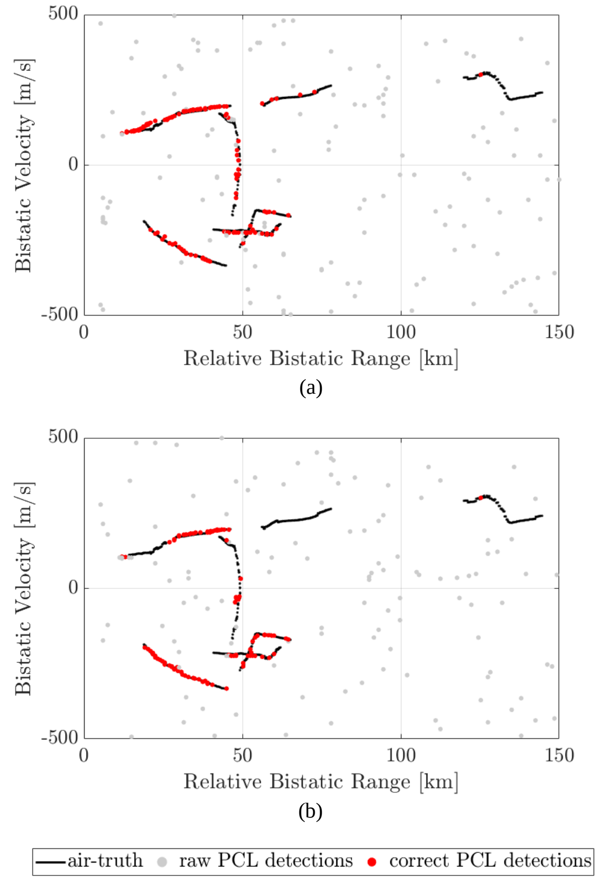

Fig.4 Raw detections for 40 consecutive data files with $P_{FA} = 10^{-4}$, using (a) single-pol channel H; (b) single-pol channel V

In fact, a number of additional plots is obtained in almost every track. The advantage is particularly evident on the track at [55-75] km and at approx. 250 m/s, which is detected with good continuity only when using the proposed strategy. Additionally, with reference to the track at [120-140] km, we notice that even though the proposed approach still fails to detect it at some data files, the number of detections obtained with the Pol-AR-AMF is twice as high as with the Pol-GLRT and more than tripled with respect to the single-pol solutions and the Pol-NCI. Finally, the overall improvement is tremendous if compared to Fig.4 (a-b) and Fig.5(a).

The preliminary results in Fig.3-Fig.5 have shown that the proposed Pol-AR-AMF strategy is able to effectively reject the disturbance limiting target detection, by jointly exploiting its statistical characteristics, both in polarization and in time domain. It is worth noticing that in this work we only reported the results for one illustrative value of the parameter Q, whose selection is the result of a trade-off between the obtained performance and the required computational load.

However, some issues are left open and further investigations are needed. They will be briefly discussed in the following Section.

IV. OPEN ISSUES AND FUTURE CHALLENGES

In order to assess the performance of the proposed detection strategy, a number of tests over the entire data set must be carried out. Specifically, an extensive analysis that aims at investigating the impact on the final performance of essential parameters, such as the AR filter order to be used. Nevertheless, the high computational burden required by the direct implementation of the proposed detector would make the aforementioned extensive analyses unsuitable.

Therefore, future works will address possible strategies that aim at reducing the computational load while accepting small losses. Such advancement would also allow extending the proposed adaptive detector to a multi-frequency scenario. In fact, it was shown in [10] that polarimetric and frequency diversity can be fruitfully jointly exploited to further improve the target detection capability.

V. CONCLUSIONS

In this work, we presented a novel polarimetric adaptive detection algorithm for PCL systems based on a 2D auto-regressive model for the disturbance.

Thanks to the availability of experimental data, collected with a FM radio-based PCL multi-channel receiver, we demonstrated that the proposed approach is able to effectively counteract the disturbance affecting the surveillance signals, hence enhancing the target detection capability. Moreover, some limitations and open issue have also been identified and will be addressed in future works.

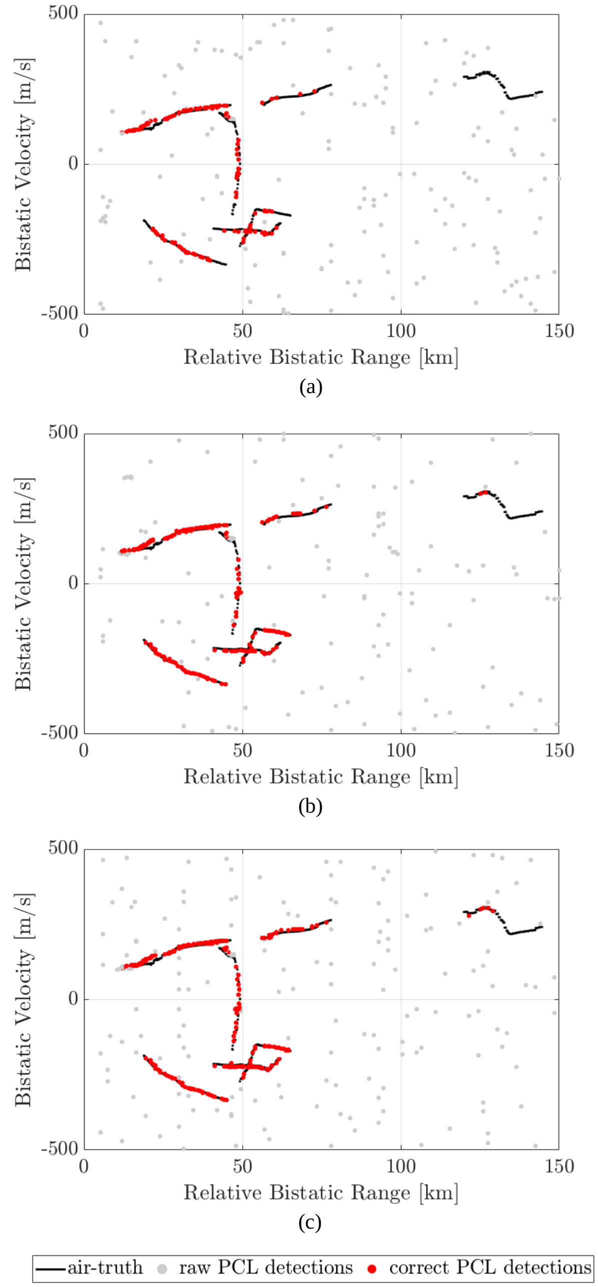

Fig.5 Raw detections for 40 consecutive data files with $P_{FA} = 10^{-4}$, using (b) Pol-NCI; (b) Pol-GLRT; (c) Pol-AR-AMF with Q = 5

REFERENCES

[1] A. Farina, H. Kuschel : IEEE Aerospace and Electronic Systems Magazine, Special Issue on Passive Radar, Part I & II, 27, (10-11), October 2012.

[2] K.E. Olsen, H. Kuschel : IEEE Aerospace and Electronic Systems Magazine, Special Issue : Passive and Multi-Static Radar for Civil Applications, 32, (2), February 2017.

[3] P. E. Howland, D. Maksimiuk and G. Reitsma, "FM radio based bistatic radar," in *IEE Proceedings - Radar, Sonar and Navigation*, vol. 152, no. 3, pp. 107-115, 3 June 2005.

[4] H. Griffiths and C. Baker, "The Signal and Interference Environment in Passive Bistatic Radar," *2007 Information, Decision and Control*, Adelaide, Qld., 2007, pp. 1-10

[5] C. Bongioanni, F. Colone, T. Martelli, R. Angeli, P. Lombardo, "Exploiting polarimetric diversity to mitigate the effect of interferences in FM-based passive radar", in Proceedings of International Radar Symposium (IRS), June 2010, pp. 1-4.

[6] M. Conti, C. Moscardini and A. Capria, "Dual-polarization DVB-T passive radar: Experimental results," *2016 IEEE Radar Conference (RadarConf)*, Philadelphia, PA, 2016, pp. 1-5.

[7] F. Colone, P. Lombardo: "Polarimetric passive coherent location", IEEE Transactions on Aerospace and Electronic Systems, 2015, 51, (2), pp. 1079–1097.

[8] F.Filippini, F.Colone, D.Cristallini, G.Bournaka: "Experimental results of Polarimetric Detection Schemes for DVB-T based Passive Radar", IET Radar, Sonar & Navigation, 2017, 11 (6), pp. 883-891

[9] F. Filippini and F. Colone, "A practical approach to polarimetric adaptive target detection in passive radar," *International Conference on Radar Systems (Radar 2017)*, Belfast, 2017, pp. 1-6.

[10] F. Colone and P. Lombardo, "Non-coherent adaptive detection in passive radar exploiting polarimetric and frequency diversity," in *IET Radar, Sonar & Navigation*, vol. 10, no. 1, pp. 15-23, 1 2016.

[11] F. Colone, C. Palmarini, . Martelli and E. Tilli, "Sliding extensive cancellation algorithm for disturbance removal in passive radar," in *IEEE Transactions on Aerospace and Electronic Systems*, vol. 52, no. 3, pp. 1309-1326, June 2016.